Supporting Information:

Single-Molecule FRET Studies of HIV TAR-DNA Hairpin Unfolding Dynamics

Jixin Chen,[#,1†] Nitesh K. Poddar,[#,1‡] Lawrence J. Tauzin,[1] David Cooper,[1] Anatoly B. Kolomeisky,[1]

Christy F. Landes[,1,2]*

[1]Department of Chemistry, Rice University, Houston, TX 77251 (USA)

[2]Department of Electrical and Computer Engineering, Rice University, Houston, TX 77251 (USA)

† Current address: Department of Chemistry and Biochemistry, Ohio University, Athen, Ohio 45701

‡ Current address: Department of Biotechnology, IIET, Invertis University, Bareilly-243123, (INDIA)

[#] J.C and N.K.P. contributed equally.

[*] e-mail: cflandes@rice.edu

Contents

1. Additional experimental methods

Circular Dichroism (CD) Measurements. Isothermal far-UV spectra of all DNAs were measured at 20 °C in a Jasco spectropolarimeter (model J-815) equipped with a Peltier type temperature controller (PFD-425S/15). DNA concentration used for the CD measurements was in the range of 200-400 µM. Cells of 0.1 cm path length were used for the measurements of the far-UV spectra. The CD instrument was routinely calibrated with D-10-camphorsulfonic acid. The results of all the CD measurements are expressed as mean residue ellipticity ($[\theta]_\lambda$) in deg cm^2 mol^{-1} at a given wavelength λ (nm) using the relation.[1-2]

$$[\theta]_\lambda = \frac{\theta_\lambda M_0}{10\ cl} \qquad \text{(S1)}$$

where θ_λ is the observed ellipticity in millidegrees at wavelength λ, M_0 is the mean molar residue weight of the DNA in g/mol, c is the protein concentration (mg/cm^3), and l is the path length (cm). Each observed θ_λ of the DNA was corrected for the contribution of the solvent.

Time-Resolved Fluorescence Anisotropy Measurements. Fluorescence lifetime and anisotropy measurements were performed on all three DNA constructs in this study to verify that the changes in the measured FRET efficiencies were not due to unwanted photophysics or on decreased rotational freedom of the dyes. The data were acquired using a Fluotime 300 (Picoquant, Germany) using a 640 nm pulsed diode laser excitation source PDL-D-C 640 (Picoquant, Germany) driven by a PDL 820 (Picoquant, Germany) laser driver. The emission monochromator was set to 670 nm. Photons were detected using a PMT model PMA-C 182-N-M (Picoquant, Germany). The instrument response function (IRF) was measured using a scattering solution (Ludox colloidal silica, Sigma). The measured full width at half maximum (FWHM) of the lifetime of the excitation laser was about 50 ps. The concentration of the constructs used for these measurements was 100 nM.

2. Labeling strategy

There are multiple considerations for choosing a dye labeling strategy for biomolecules. First, it must be demonstrated that the labeling chemistry minimally influences the biochemical system under evaluation. This has been accomplished by a combination of the circular dichroism analysis summarized in Section S2, biological assays that maintain strand transfer efficiency in the case of the present TAR DNA hairpin,[3-8] and structural analyses such as NMR characterization.[9-11] The Cy3/Cy5 pair has been widely studied in DNA labeling and results in reduced effects on the DNA dynamics among several choices of dyes.[12-13]

Next, it is necessary to ensure that the biochemical functionalization does not induce significant biochemical or biophysical effects on the observed dye characteristics. In the present study, this has been accomplished by including thymidine spacers at each hairpin terminus, in order to prevent the stacking of these dyes with the nucleotide bases. Studies have shown that Cy3 and Cy5 dyes will stack with terminal bases in double-stranded DNA, limiting dye rotational mobility.[9, 14-15] This effect can be corrected by including an orientation factor of the dyes,[14-16] but this correction introduces difficulties in identifying different states due to the smaller variations of the FRET efficiencies. For the current dye-hairpin combination, the effectiveness of thymidine spacers at minimizing unwanted interactions between the

dyes, the linkers, and the DNA has been demonstrated extensively[3-8], and in the current work, this interpretation is further confirmed by the fluorescence lifetime, rotational anisotropy, and photon count analyses in section S3.

Finally, it is important, in the case of FRET, to establish that the reported photon counts from the donor and acceptor are anticorrelated and are genuinely reflective of the relevant distance changes in the biomolecule. There are three strategies by which this concern is addressed in the current work. (1) The chosen labeling strategy has been demonstrated to be an effective way to measure the length of the single-stranded DNA (ssDNA) that connects the Cy3 and Cy5 dyes.[17-18] The optimized choice of the linkers and dyes has also been confirmed by recent theoretical and experimental studies.[9, 13] (2) The choice of well-established labeling protocols is further tested by a cross-correlation test of every single molecule smFRET trajectory, demonstrating that, on average, ~5% of selected molecules are rejected because of positive cross-correlation (data not shown). This provides experimental support that the collected photons from Cy5 can only be due to energy transfer between Cy3 and Cy5. (3) Finally the thymidine spacer length at the ends of the TAR-DNA hairpin were optimized such that the expected intramolecular end distances correspond to the maximum dynamic range of FRET values predicted for the Cy3/Cy5 FRET pair.

As mentioned above, the extended 4-dT spacer between the Cy5 and the ssDNA serves an additional purpose beyond preventing dye-base stacking. The extension shifts and optimizes the average separation distances to the dynamic range of the Förster relationship between distance and FRET dependence for Cy3-Cy5 dyes of between ~3 nm to ~12 nm (**Figure S1**).

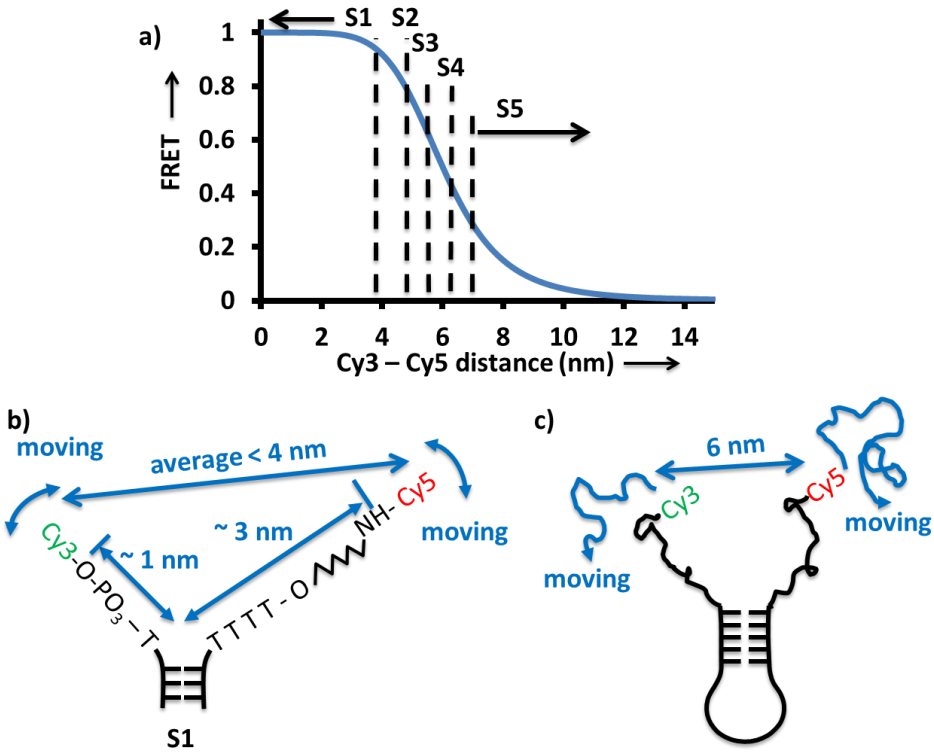

Figure S1. Scheme of the FRET between Cy3 and Cy5 for TAR-DNA. (a) Dependence of FRET efficiency on the dye-dye distance assuming R_0 = 6.0 nm,[14, 17] when the average orientation factor is used for the calculation. (b) State S1 of the TAR DNA hairpin in the manuscript and the labeling geometry of the dyes. (c) Scheme of State S4 and the motion of the ends of the DNA hairpin.

3. Theoretical calculation of open and closed lifetime of DNA hairpin loops

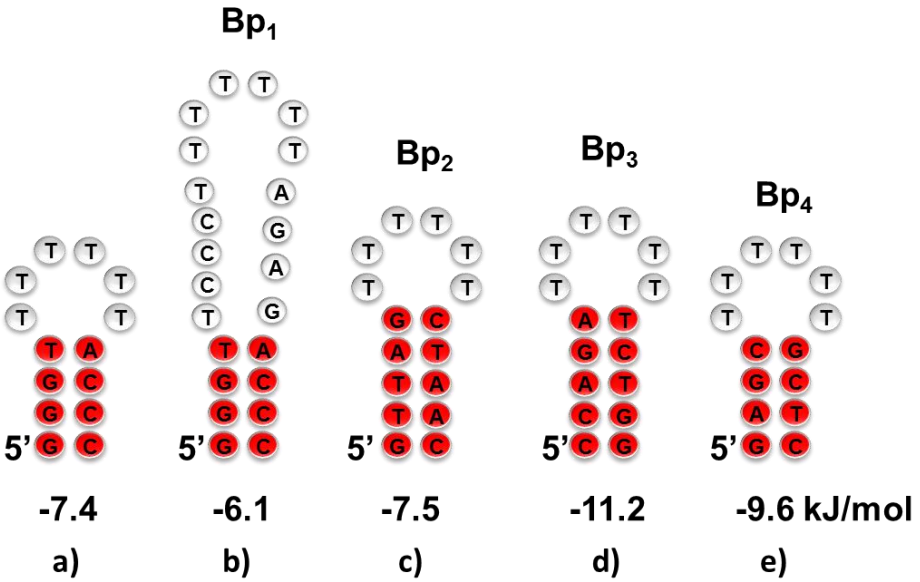

Figure S2. Calculated formation free energy of the paired regions of TAR DNA, Bp_n, by Mfold (conditions: 40 mM Na^+, and 20 ^oC). Six dT are added to each Bp_n for consistence

The possible secondary structures and formation free energy, ΔG_{closed} of one-loop opened and two-loop opend TAR-DNA are calculated by Mfold[19] (**Figure S2**) with the rest of the trunk part deleted, and 6 dT added for the ease of calculation. Mfold is based on the nearest-neighbor method.[19-22] The open and close lifetime are calculated with the model developed by Grunwell *et al.*[23] and Bonnet *et al.*[24]. The equilibrium constant from the open state to the closed-state, K_{closed} at room temperature are caculated by **Equation S2** from the free energy. The closing rate k_{close} of hairpin of given loop size and basepair, k_{open} are determined by the calibration slop measured by Bonnet *et al.*[24] Then the opening rate constant of the DNA-hairpin is calculated from **Equation S3** (**Table S1**).

$$\Delta G_{closed} = -RTln(K_{closed}) \qquad \text{(S2)}$$

$$K_{closed} = k_{close}/k_{open} \qquad \text{(S3)}$$

Most lifetimes ($1/k_{open}$) of the open states of the hairpins in **Figure S2** are estimated around 10 μs time scale, and the lifetimes of the closed states are at 1 ms time scale.

Table S1. Rough estimation of the opening and closing lifetimes of the hairpins in **Figure S2**

	a	b	c	d	e
ΔG_{closed} (kJ/mol)	−7.4	−6.1	−7.5	−11.2	−9.6
K_{closed}	20.8	12.2	21.7	98.7	51.2
k_{close} (s^{-1})*	5.5×10^4	2.1×10^4	5.4×10^4	5.4×10^4	5.5×10^4
k_{open} (s^{-1})	2.6×10^3	1.7×10^3	2.5×10^3	5.5×10^2	1.1×10^3

* Literature values from Bonnet *et al.*[24]

4. Photophysics of Cy3 and Cy5

The time-resolved fluorescence data (**Table S2**) were acquired from the fluorescence lifetime and anisotropy measurements carried out for the acceptor dye (Cy5) on all the constructs of the DNA in the presence and absence of PEG and urea. **Table S2** shows the fluorescence lifetime and anisotropy measurements of the Cy5 dye conjugated with all constructs of the DNA (**Figure S3**). As is seen in **Table**

S2, the average fluorescence lifetimes of all the Cy5-DNAs are within the range of 1.0 ns to 1.3 ns irrespective of the solutions, which is in good agreement with the reported values.[25] Also, the average rotational lifetimes of all the Cy5-DNAs are in the range of 0.5 ns to 2.0 ns range (**Table S2**). Moreover, when PEG was added, the lifetime of the Cy5 dye has a fast component at ~0.1 ns and another major component at ~1.7 ns. This fast component might arise from slowing down of otherwise unobservable fast movement of the dye molecules without PEG molecules. Nevertheless, these results do not support the assumption that the photophysics of the dye molecules were significantly changed by PEG molecules since the fluorescence lifetime remains unchanged. The slight slowing down of the rotation will not affect our FRET measurement since there is a few orders of magnitude difference in the time scale, as the rotational lifetimes are in the ns time scale and our smFRET data are compared at 10 ms integration time. Thus, we conclude that the broadening of the smFRET distribution we see for the TAR-DNA hairpin, and to a lesser extent for the mutants, is due to a new ability, in the viscous PEG solution, to observe loop-open states that ordinarily have lifetimes that are too short for us to detect.

Table S2. Photophysical properties of Cy5-DNA

sample	condition	fluorescence lifetimes					rotational lifetimes				
		τ_1 (ns)	τ_2 (ns)	f_1 (%)	f_2 (%)	τ_{avg} (ns)	φ_1 (ns)	φ_2 (ns)	f_1' (%)	f_2' (%)	φ_{avg} (ns)
TAR	buffer	1.25	0.63	75	25	1.10	1.5	-	100	-	1.5
	6M urea	1.21	-	100	-	1.21	0.72	-	100	-	0.72
	24% PEG	1.41	0.04	91	9	1.29	1.84	0.08	98	2	1.81
	20% PEG + 6M urea	1.40	0.61	95	5	1.36	1.65	0.10	95	5	1.58
mutant	buffer	1.30	0.68	58	42	1.04	0.54	-	100	-	0.54
	6M urea	1.18	-	100	-	1.18	1.00	-	100	-	1.00
	24% PEG	1.45	0.03	94	6	1.20	1.70	0.08	93	7	1.59
	20% PEG + 6 M urea	1.38	-	100	-	1.38	1.65	0.10	95	5	1.57

f_1, f_2 & f_1', f_2' are fractions contributed to fluorescence lifetimes and rotational lifetimes, respectively.

Samp. means Samples; Cond. means Conditions. Buffer means HEPES buffer (25 mM) and NaCl (40 mM) plus oxygen scavenging solution. They were added in all the other conditions too.

τ_{avg} & φ_{avg} are average florescence lifetime and rotational life time, respectively.

$\tau_{avg} = \Sigma\alpha_i\tau_i^2/\Sigma\alpha_i\tau_i$ and $\varphi_{avg} = \Sigma b_i\varphi_i^2/\Sigma b_i\varphi_i$ where a and b are the pre-exponential factors of the fitting.[26]

$f_i = \alpha_i\tau_i/\Sigma\alpha_i\tau_i$ and $f_i' = b_i\varphi_i/\Sigma b_i\varphi_i$.[26]

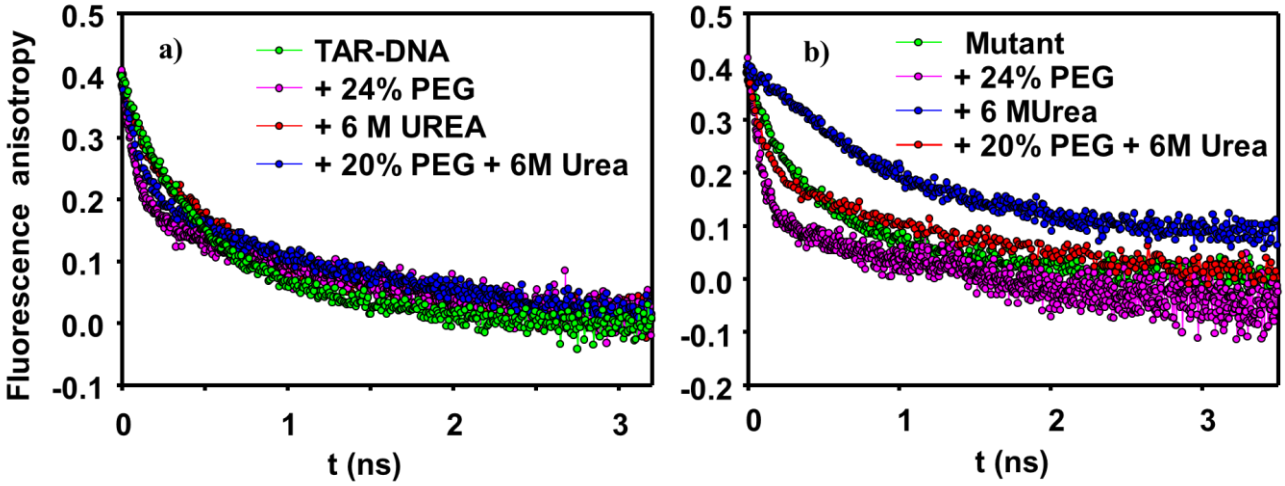

Figure S3. Time-resolved Cy5 fluorescence anisotropy measurements of (a) TAR-DNA, and (b) mutant DNA with time correlated single photon counting (TCSPC) lifetime spectroscopy. Fitting parameters are listed in **Table S2**.

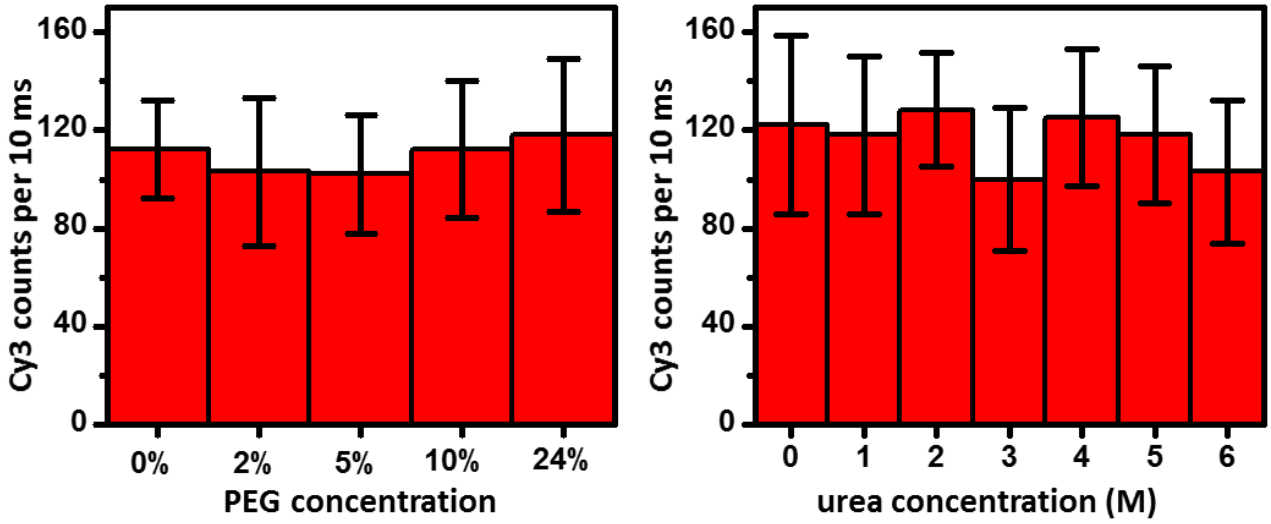

Figure S4. Single-molecule photon-counts of Cy3 attached to TAR-DNA (immobilized on the PEG-glass slides) under different PEG-6000 concentrations (left) and urea concentrations (right). Each plot was done within the same day. Oxygen scavenger, other buffer conditions and the excitation laser intensity were maintained the same for all the measurements. The error bars are the standard deviation of the average photon-counts of ~20 molecules

Figure S4 supports the assumption that the photo-physics of the Cy3 donor dye are the same in solutions with different concentrations of PEG-6000 and urea under our experimental conditions. First, the average single-molecule photon-counts of the Cy3 donor dye remain the same in different solutions under the same excitation intensity. Second, the consistent amplitudes of the error bars indicate similar behavior of the Cy3 dye in different solutions. The error bars are mainly due to the strong environmental dependence of the Cy3 dye and the variation of the local environment of the molecules on the substrates, which is consistent with the results observed by others in the literature.[12]

5. TAR DNA dynamics under PEG

We confirmed that PEG-6000 has negligible effects on the secondary structure of DNA and the dye photophysical response using circular dichroism (CD) (**Figure S5**) and fluorescence anisotropy decay measurements for all the constructs of DNAs in the presence and absence of PEG (**Figure S3**). Therefore, we considered PEG-6000 a suitable crowding agent to slow down the dynamics of the TAR-DNA and mutant constructs.

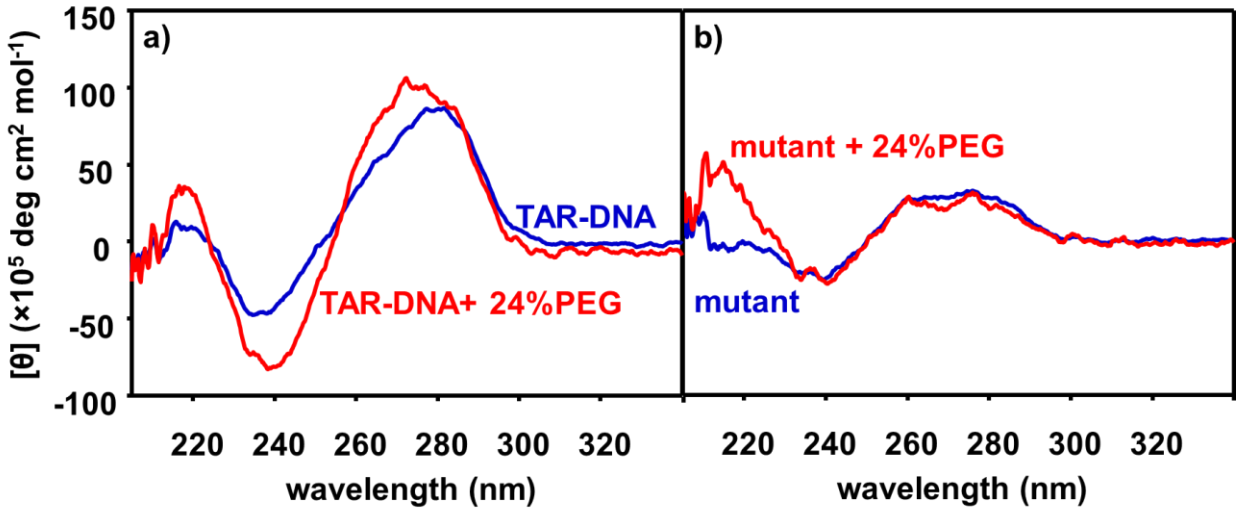

Figure S5. Circular dichroism spectra of the nucleotides of the (a) TAR-DNA, (b) mutant in the presence and absence of 24% wt of PEG solution.

By analyzing the dwell times for transitions between the state S_1 and S_2 identified by HaMMy,[27] (**Figure S6**) we can confirm that the addition of PEG slows down the opening and closing dynamics of the DNA hairpin. The lifetimes of state S_1 and state S_2 of TAR-DNA hairpin, 353 ms and 142 ms respectively, are slower by two orders and four orders of magnitude respectively in the presence of PEG as compared to the theoretical values in the absence of PEG mentioned earlier. This indicates that the decrease in configurational diffusion in the presence of PEG has a greater effect on the closing rate than the opening rate, yielding an equilibrium distribution that is shifted slightly away from the closed hairpin distribution.[28-29] Based on these results, we conclude that PEG alone is insufficient to allow us to observe the other three open states S_3, S_4, and S_5 of TAR DNA.

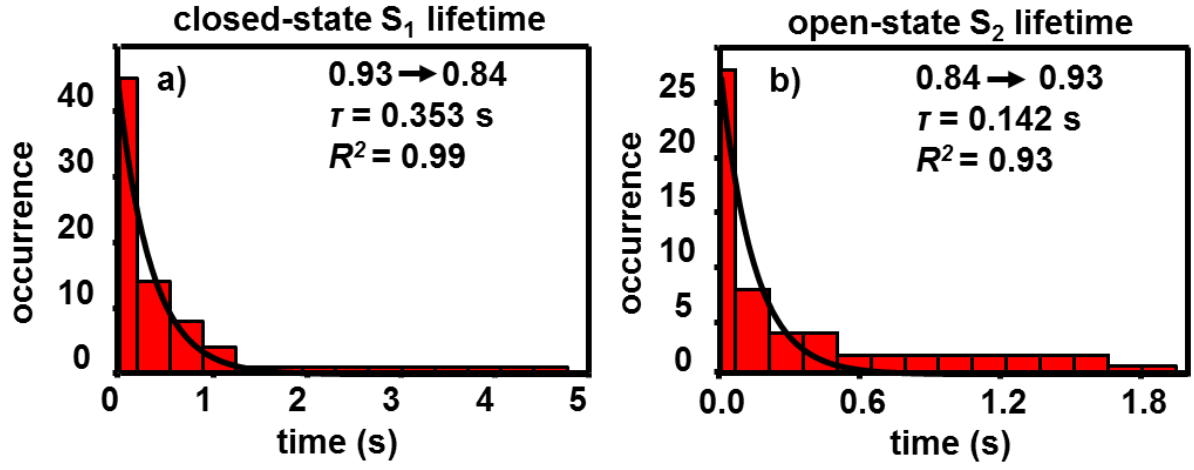

Figure S6. Dwell-time histograms of TAR-DNA at 24% PEG condition using hidden Markov model

(HMM).30-32 (A) and (B) represent the exponential fits to 2-state opening and closing of the hairpin using HMM. Transitions to the state at FRET efficiency ~0.45 (Figure 3d in the main text) were not analyzed because only 2 of the 74 analyzed molecules exhibited this state. This rare occurrence could either be due to misfolding during the reannealing process or to the proposed breaking of ergodicity for single molecules,[33] and perhaps deserves more detailed future treatment, but either is outside the current statistical treatment.

6. Full trajectories of data in main text Figure 3d and Figure 6

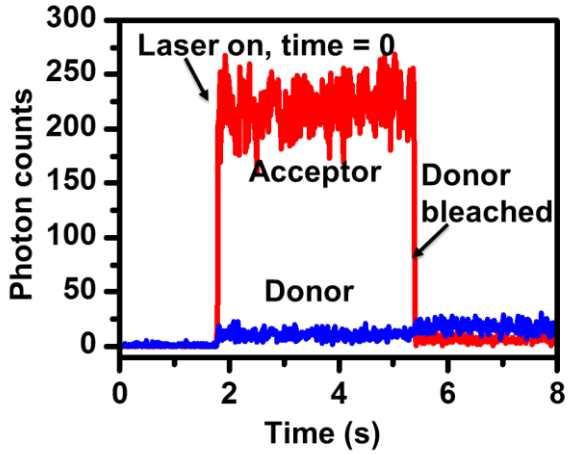

Figure S7. Time trajectory of the data in main text Figure 3d.

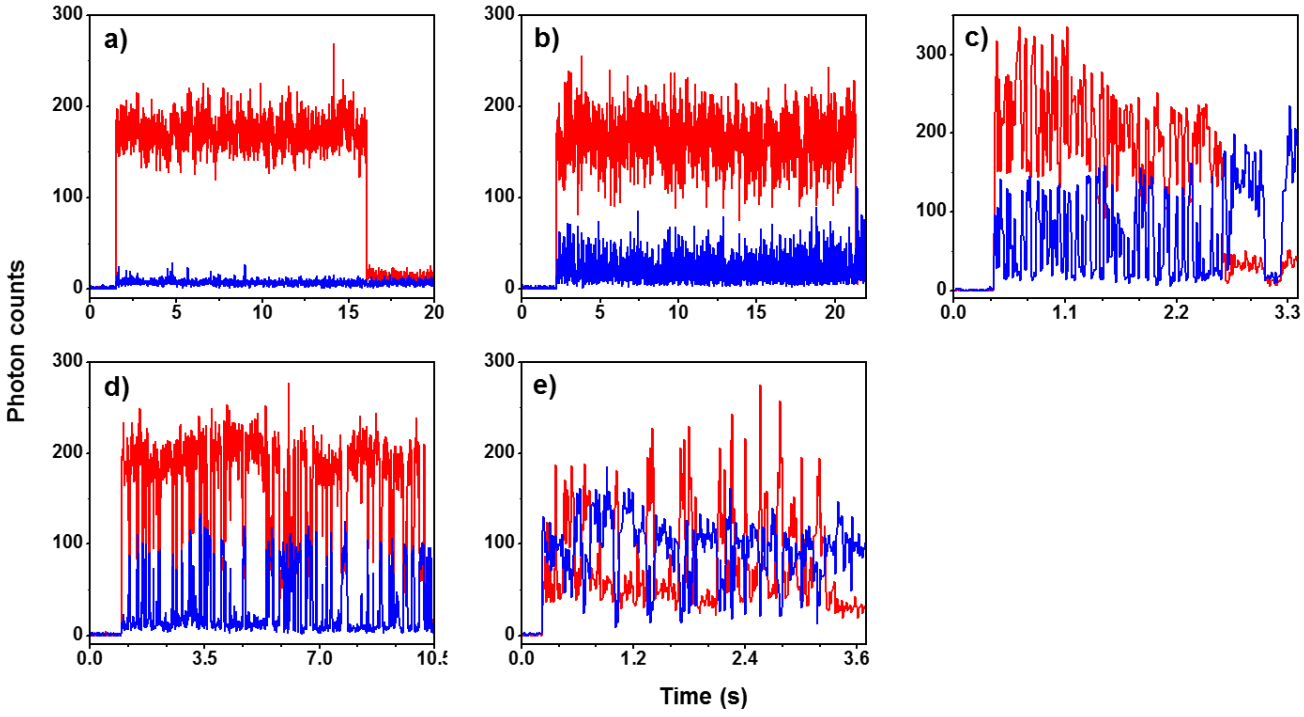

Figure S8. Time trajectories of the data in main text Figure 6 in the same order.

7. Conclusion remarks

We expect that this work will have the following impacts: (1) We conclude that a possible biological function for a hairpin loop is to serve as an additional fraying center to increase opening rates in otherwise stable systems; such insight into loop function could help both DNA-targeting therapeutic and

biosensing systems that are highly dependent on DNA dynamics.[34-39] (2) We suggest practical strategies to obtain the kinetic and thermodynamic information from single-molecule experiments. (3) Combination of PEG and urea will further increase our ability to study the detailed kinetics of each step and will be conducted in the future. A preliminary study (**Figure S9**) has shown promising results that more populations on the lower FRET region are observed by adding 10% PEG into the 5 M urea buffer solution. We will carry out further systematic studies and build devices to tune the temperatures in the future. (4) We expect the experimental and kinetic analytical approaches developed in this article to provide useful tools in studying the mechanism of multi-state DNA hairpin dynamics, or other general systems with multiple parallel pathways of chemical reactions, especially when non-equilibrium states are difficult to achieve, which prohibits any ensemble method to measure the kinetics.

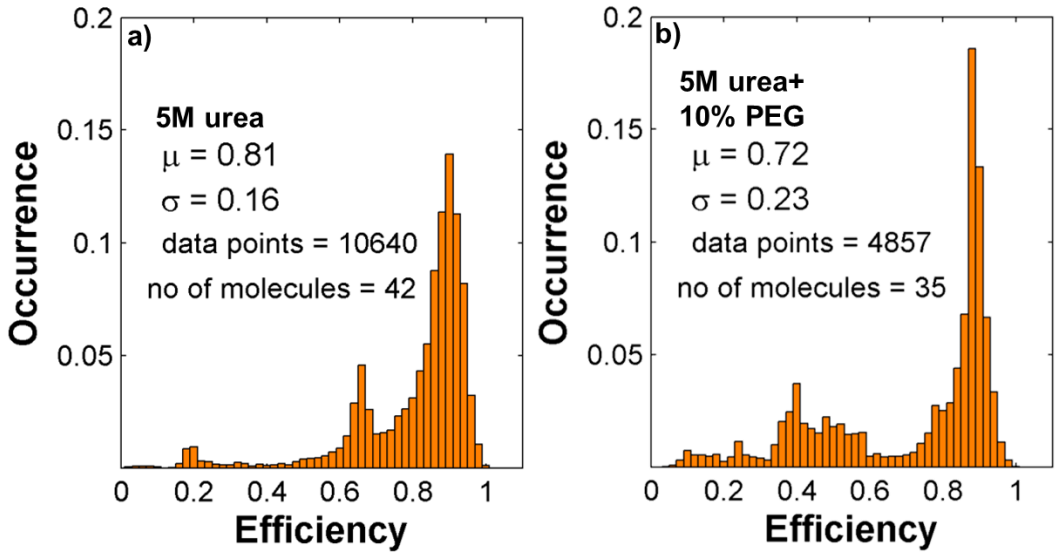

Figure S9. Global ensemble histogram of TAR-DNA in the presence and absence of 10% PEG and 5M Urea. Inset also shows the mean FRET efficiency (μ) and standard deviation (σ) of the histogram.

References

(1) Kelly, S. M.; Price, N. C. The Use of Circular Dichroism in the Investigation of Protein Structure and Function. *Curr. Protein Pept. Sci.* **2000,** *1*, 349-384.

(2) Poddar, N. K.; Ansari, Z. A.; Singh, R. K.; Moosavi-Movahedi, A. A.; Ahmad, F. Effect of Monomeric and Oligomeric Sugar Osmolytes on Deltagd, the Gibbs Energy of Stabilization of the Protein at Different pH Values: Is the Sum Effect of Monosaccharide Individually Additive in a Mixture? *Biophys. Chem.* **2008,** *138*, 120-9.

(3) Hong, M. K.; Harbron, E. J.; O'Connor, D. B.; Guo, J.; Barbara, P. F.; Levin, J. G.; Musier-Forsyth, K. Nucleic Acid Conformational Changes Essential for HIV-1 Nucleocapsid Protein-Mediated Inhibition of Self-Priming in Minus-Strand Transfer. *J. Mol. Biol.* **2003,** *325* (1), 1–10.

(4) Cosa, G.; Harbron, E. J.; Zeng, Y.; Liu, H.-W.; O Connor, D. B.; Eta-Hosokawa, C.; Musier-Forsyth, K.; Barbara, P. F. Secondary Structure and Secondary Structure Dynamics of DNA Hairpins Complexed with HIV-1 NC Protein. *Biophys. J.* **2004,** *87* (4), 2759–2767.

(5) Liu, H. W.; Cosa, G.; Landes, C. F.; Zeng, Y.; Kovaleski, B. J.; Mullen, D. G.; Barany, G.; Musier-Forsyth, K.; Barbara, P. F. Single-Molecule FRET Studies of Important Intermediates in the Nucleocapsid-Protein-Chaperoned Minus-Strand Transfer Step in HIV-1 Reverse Transcription. *Biophys. J.* **2005,** *89*, 3470–3479.

(6) Cosa, G.; Zeng, Y.; Liu, H. W.; Landes, C. F.; Makarov, D. E.; Musier-Forsyth, K.; Barbara, P. F. Evidence for Non-Two-State Kinetics in the Nucleocapsid Protein Chaperoned Opening of DNA Hairpins. *J. Phys. Chem. B* **2006,** *110*, 2419–2426.

(7) Landes, C. F.; Zeng, Y.; Liu, H.-W.; Musier-Forsyth, K.; Barbara, P. F. Single-Molecule Study of the Inhibition of HIV-1 Transactivation Response Region DNA/DNA Annealing by Argininamide. *J. Am. Chem. Soc.* **2007,** *129*, 10181–10188.

(8) Liu, H.-W.; Zeng, Y.; Landes, C. F.; Kim, Y. J.; Zhu, Y.; Ma, X.; Vo, M.-N.; Musier-Forsyth, K.; Barbara, P. F. Insights on the Role of Nucleic Acid/Protein Interactions in Chaperoned Nucleic Acid Rearrangements of HIV-1 Reverse Transcription. *Proc. Natl. Acad. Sci. U.S.A.* **2007,** *104*, 5261-5267.

(9) Spiriti, J.; Binder, J. K.; Levitus, M.; van der Vaart, A. Cy3-DNA Stacking Interactions Strongly Depend on the Identity of the Terminal Basepair. *Biophys. J.* **2011,** *100* (4), 1049-1057.

(10) Iqbal, A.; Wang, L.; Thompson, K. C.; Lilley, D. M. J.; Norman, D. G. The Structure of Cyanine 5 Terminally Attached to Double-Stranded DNA: Implications for FRET Studies. *Biochemistry* **2008,** *47* (30), 7857-7862.
(11) Urnavicius, L.; McPhee, Scott A.; Lilley, David M. J.; Norman, David G. The Structure of Sulfoindocarbocyanine 3 Terminally Attached to Dsdna Via a Long, Flexible Tether. *Biophys. J.* **2012,** *102* (3), 561-568.
(12) Ha, T.; Tinnefeld, P. Photophysics of Fluorescent Probes for Single-Molecule Biophysics and Super-Resolution Imaging. *Annu. Rev. Phys. Chem.* **2012,** *63* (1), 595–617.
(13) Di Fiori, N.; Meller, A. The Effect of Dye-Dye Interactions on the Spatial Resolution of Single-Molecule FRET Measurements in Nucleic Acids. *Biophys. J.* **2010,** *98* (10), 2265-2272.
(14) Iqbal, A.; Arslan, S.; Okumus, B.; Wilson, T. J.; Giraud, G.; Norman, D. G.; Ha, T.; Lilley, D. M. J. Orientation Dependence in Fluorescent Energy Transfer between Cy3 and Cy5 Terminally Attached to Double-Stranded Nucleic Acids. *Proc. Natl. Acad. Sci. U.S.A.* **2008,** *105* (32), 11176–11181.
(15) Ouellet, J.; Schorr, S.; Iqbal, A.; Wilson, Timothy J.; Lilley, David M. J. Orientation of Cyanine Fluorophores Terminally Attached to DNA Via Long, Flexible Tethers. *Biophys. J.* **2011,** *101* (5), 1148-1154.
(16) Sindbert, S.; Kalinin, S.; Nguyen, H.; Kienzler, A.; Clima, L.; Bannwarth, W.; Appel, B.; Müller, S.; Seidel, C. A. M. Accurate Distance Determination of Nucleic Acids Via Förster Resonance Energy Transfer: Implications of Dye Linker Length and Rigidity. *J. Am. Chem. Soc.* **2011,** *133* (8), 2463-2480.
(17) Murphy, M. C.; Rasnik, I.; Cheng, W.; Lohman, T. M.; Ha, T. Probing Single-Stranded DNA Conformational Flexibility Using Fluorescence Spectroscopy. *Biophys. J.* **2004,** *86* (4), 2530–2537.
(18) Chen, H.; Meisburger, S. P.; Pabit, S. A.; Sutton, J. L.; Webb, W. W.; Pollack, L. Ionic Strength-Dependent Persistence Lengths of Single-Stranded RNA and DNA. *Proc. Natl. Acad. Sci. U.S.A.* **2012,** *109* (3), 799-804.
(19) Zuker, M. Mfold Web Server for Nucleic Acid Folding and Hybridization Prediction. *Nucleic Acids Res.* **2003,** *31*, 3406-15.
(20) Breslauer, K. J.; Frank, R.; Blöcker, H.; Marky, L. A. Predicting DNA Duplex Stability from the Base Sequence. *Proc. Natl. Acad. Sci. U.S.A.* **1986,** *83*, 3746-3750.
(21) SantaLucia, J.; Allawi, H. T.; Seneviratne, P. A. Improved Nearest-Neighbor Parameters for Predicting DNA Duplex Stability. *Biochemistry* **1996,** *35*, 3555-3562.
(22) SantaLucia, J. A Unified View of Polymer, Dumbbell, and Oligonucleotide DNA Nearest-Neighbor Thermodynamics. *Proc. Natl. Acad. Sci. U.S.A.* **1998,** *95*, 1460-1465.
(23) Grunwell, J. R.; Glass, J. L.; Lacoste, T. D.; Deniz, A. A.; Chemla, D. S.; Schultz, P. G. Monitoring the Conformational Fluctuations of DNA Hairpins Using Single-Pair Fluorescence Resonance Energy Transfer. *J. Am. Chem. Soc.* **2001,** *123*, 4295–4303.
(24) Bonnet, G.; Krichevsky, O.; Libchaber, A. Kinetics of Conformational Fluctuations in DNA Hairpin-Loops. *Proc. Natl. Acad. Sci. U.S.A.* **1998,** *95*, 8602–8606.
(25) Schobel, U.; Egelhaaf, H. J.; Brecht, A.; Oelkrug, D.; Gauglitz, G. New Donor-Acceptor Pair for Fluorescent Immunoassays by Energy Transfer. *Bioconjug. Chem.* **1999,** *10*, 1107-14.
(26) Lakowicz, J. R., In *Principles of Fluorescence Spectroscopy*, 4th ed.; Springer Science+Business Media, LLC: New York, NY, 2010.
(27) McKinney, S. *http://bio.physics.uiuc.edu/ HaMMy 2006*, (accessed 12/2012).
(28) Ansari, A.; Kuznetsov, S. V.; Shen, Y. Configurational Diffusion Down a Folding Funnel Describes the Dynamics of DNA Hairpins. *Proc. Natl. Acad. Sci. U.S.A.* **2001,** *98*, 7771–7776.
(29) Ansari, A.; Shen, Y.; Kuznetsov, S. V. Misfolded Loops Decrease the Effective Rate of DNA Hairpin Formation. *Phys. Rev. Lett.* **2002,** *88*, 069801.
(30) Andrec, M.; Levy, R. M.; Talaga, D. S. Direct Determination of Kinetic Rates from Single-Molecule Photon Arrival Trajectories Using Hidden Markov Models. *J. Phys. Chem. A* **2003,** *107* (38), 7454–7464.
(31) Talaga, D. S. Markov Processes in Single Molecule Fluorescence. *Curr. Opin. Colloid Interface Sci.* **2007,** *12* (6), 285–296.
(32) McKinney, S. A.; Joo, C.; Ha, T. Analysis of Single-Molecule FRET Trajectories Using Hidden Markov Modeling. *Biophys. J.* **2006,** *91*, 1941–1951.
(33) Hyeon, C.; Lee, J.; Yoon, J.; Hohng, S.; Thirumalai, D. Hidden Complexity in the Isomerization Dynamics of Holliday Junctions. *Nat. Chem.* **2012,** *4* (11), 907-914.
(34) Bayley, H.; Cremer, P. S. Stochastic Sensors Inspired by Biology. *Nature* **2001,** *413*, 226-230.
(35) Smith, E. A.; Kyo, M.; Kumasawa, H.; Nakatani, K.; Saito, I.; Corn, R. M. Chemically Induced Hairpin Formation in DNA Monolayers. *J. Am. Chem. Soc.* **2002,** *124* (24), 6810-6811.
(36) Radi, A.-E.; Acero Sánchez, J. L.; Baldrich, E.; O'Sullivan, C. K. Reagentless, Reusable, Ultrasensitive Electrochemical Molecular Beacon Aptasensor. *J. Am. Chem. Soc.* **2005,** *128*, 117-124.
(37) Cutler, J. I.; Auyeung, E.; Mirkin, C. A. Spherical Nucleic Acids. *J. Am. Chem. Soc.* **2012,** *134* (3), 1376-1391.
(38) Peh, W. Y. X.; Reimhult, E.; Teh, H. F.; Thomsen, J. S.; Su, X. Understanding Ligand Binding Effects on the Conformation of Estrogen Receptor A-DNA Complexes: A Combinational Quartz Crystal Microbalance with Dissipation and Surface Plasmon Resonance Study. *Biophys. J.* **2007,** *92*, 4415-4423.
(39) Kohler, J. J.; Schepartz, A. Kinetic Studies of Fos.Jun.DNA Complex Formation: DNA Binding Prior to Dimerization. *Biochemistry* **2000,** *40* (1), 130-142.